Inorg. Chem. **2007**, *46*, 6129–6135

Low-Valence Triruthenium Compounds via Substitution of a Bridging Acetate in the Parent $Ru_3O(OAc)_6$ Cluster Core by 2,2′-Azobispyridine (abpy) or 2,2′-Azobis(5-chloropyrimidine) (abcp)

Heng-Yun Ye,[†] Feng-Rong Dai,[†] Li-Yi Zhang,[†] and Zhong-Ning Chen*[,†,‡]

State Key Laboratory of Structural Chemistry, Fujian Institute of Research on the Structure of Matter, The Chinese Academy of Sciences, Fuzhou, Fujian 350002, China, and Key State Laboratory of Coordination Chemistry, Nanjing University, Nanjing 210093, China

Received February 12, 2007

Reaction of oxo-centered $Ru_3^{III,III,III}$ precursor $[Ru_3O(OAc)_6(py)_2(CH_3OH)](PF_6)$ (**1**) with 1 equiv of 2,2′-azobispyridine (abpy) or 2,2′-azobis(5-chloropyrimidine) (abcp) induced the formation of stable $Ru_3^{III,III,II}$ derivatives $[Ru_3O(OAc)_5\{\mu\text{-}\eta^1(N),\eta^2(N,N)\text{-}L\}(py)_2](PF_6)$ (L = abpy (**2**), abcp (**3**)). As established in the structure of **3** by X-ray crystallography, **2** or **3** is derived from **1** by substitution of the axial methanol and one of the bridging acetates in the parent $Ru_3O(OAc)_6$ cluster core with abpy or abcp in an $\mu\text{-}\eta^1(N),\eta^2(N,N)$ bonding mode. Reduction of **3** by hydrazine induces isolation of one-electron reduced neutral $Ru_3^{III,II,II}$ product $Ru_3O(OAc)_5\{\mu\text{-}\eta^1(N),\eta^2(N,N)\text{-abcp}\}(py)_2$ (**3a**). As revealed by electrochemical and spectroscopic studies, substituting one of the bridging acetates in the parent $Ru_3O(OAc)_6$ cluster core by abcp or abpy modifies dramatically the electronic and redox characteristics in the triruthenium derivatives. Relative to that for the parent compound $[Ru_3O(OAc)_6(py)_3](PF_6)$ ($E_{1/2}$ = –0.46 V), triruthenium-based redox potential in the redox process $Ru_3O^{III,III,III}/Ru_3O^{III,III,II}$ is significantly anodic-shifted to $E_{1/2}$ = +0.36 V for **2** and $E_{1/2}$ = +0.53 V for **3**. Furthermore, the anodic shifts of redox potentials are progressively enhanced with a decrease of the formal oxidation states in the triruthenium cluster cores. As a consequence of remarkable positive shifts for redox potentials, the low-valence $Ru_3^{III,III,II}$ and $Ru_3^{III,II,II}$ species are stabilized and accessible.

Introduction

Oxo-centered trinuclear ruthenium-carboxylate cluster compounds with general compositions $[Ru_3O(OAc)_6(L)_2L']^{n+}$ (L and L′ = axial ligand, n = 0, 1, 2) are remarkable for their rich redox and mixed-valence chemistry.[1−6] The axial ligands L are comparatively labile and readily substitutable, thus enhancing significantly the richness of triruthenium chemistry. Axial ligand substitution affords an excellent means to tune the redox levels of electron-transfer processes by introducing proper organic ligands.[7−9]

* To whom correspondence should be addressed. Fax: +86-591-8379-2346. E-mail: czn@fjirsm.ac.cn.
[†] The Chinese Academy of Sciences,.
[‡] Nanjing University.

(1) Baumann, J. A.; Salmon, D. J.; Wilson, S. T.; Meyer, T. J.; Hatfield, W. E. *Inorg. Chem.* **1978**, *17*, 3342−3350.
(2) (a) Wilson, S. T.; Bondurant, R. F.; Meyer, T. J.; Salmon, D. J. *J. Am. Chem. Soc.* **1975**, *97*, 2285−2287. (b) Baumann, J. A.; Wilson, S. T.; Salmon, D. J.; Hood, P. L.; Meyer, T. J. *J. Am. Chem. Soc.* **1979**, *101*, 2916−2920. (c) Baumann, J. A.; Salmon, D. J.; Wilson, S. T.; Meyer, T. J. *Inorg. Chem.* **1979**, *18*, 2472−2479.
(3) (a) Abe, M.; Sasaki, Y.; Yamada, Y.; Tsukahara, K.; Yano, S.; Yamaguchi, T.; Tominage, M.; Taniguchi, I.; Ito, T. *Inorg. Chem.* **1996**, *35*, 6724−6734. (b) Abe, M.; Sasaki, Y.; Yamada, Y.; Tsukahara, K.; Yano, S.; Ito, T. *Inorg. Chem.* **1995**, *34*, 4490−4498.
(4) (a) Hamaguchi, T.; Nagino, H.; Hoki, K.; Kido, H.; Yamaguchi, T.; Breedlove, B. K.; Ito, T. *Bull. Chem. Soc. Jpn.* **2005**, *78*, 591−598. (b) Salsman, J. C.; Kubiak, C. P.; Ito, T. *J. Am. Chem. Soc.* **2005**, *127*, 2382−2383.
(5) Abe, M.; Michi, T.; Sato, A.; Kondo, T.; Zhou, W.; Ye, S.; Uosaki, K.; Sasaki, Y. *Angew. Chem., Int. Ed.* **2003**, *42*, 2912−2915.
(6) Toma, H. E.; Araki, K.; Alexiou, A. D. P.; Nikolaou, S.; Dovidauskas, S. *Coord. Chem. Rev.* **2001**, *219*−*221*, 187−234.
(7) Toma, H. E.; Cunha, C. J.; Cipriano, C. *Inorg. Chim. Acta* **1988**, *154*, 63−66.
(8) (a) Ito, T.; Hamaguchi, T.; Nagino, H.; Yamaguchi, T.; Kido, H.; Zavarine, I. S.; Richmond, T.; Washington, J.; Kubiak, C. P. *J. Am. Chem. Soc.* **1999**, *121*, 4625−4632. (b) Ito, T.; Hamaguchi, T.; Nagino, H.; Yamaguchi, T.; Washington, J.; Kubiak, C. P. *Science* **1997**, *277*, 660−663. (c) Ota, K.; Sasaki, H.; Matsui, T.; Hamaguchi, T.; Yamaguchi, T.; Ito, T.; Kido, H.; Kubiak, C. P. *Inorg. Chem.* **1999**, *38*, 4070−4078. (d) Yamaguchi, T.; Imai, N.; Ito, T.; Kubiak, C. P. *Bull. Chem. Soc. Jpn.* **2000**, *73*, 1205−1212. (e) Ito, T.; Imai, N.; Yamaguchi, T.; Hamaguchi, T.; Londergan, C. H.; Kubiak, C. P. *Angew. Chem., Int. Ed.* **2004**, *43*, 1376−1381.

10.1021/ic0702771 CCC: $37.00
Published on Web 06/20/2007

In contrast with numerous investigations on axial ligand substitution chemistry in the oxo-centered triruthenium cluster compounds,[1−6,8−14] displacement of bridging acetates with organic ligands is neglected because of the high stability of the $Ru_3O(OAc)_6$ core caused by formation of six six-membered rings of the $Ru_2(O)(\mu$-OAc) moiety. In our attempt to explore the reactivity of the triruthenium precursor $[Ru_3O(OAc)_6(py)_2(CH_3OH)](PF_6)$ (**1**) with 2,2′-bipyridyl ligands, we have recently discovered that one of the bridging acetates in the parent $Ru_3O(OAc)_6$ core is substitutable with a 2,2′-bipyridyl ligand through ortho-metalation at ambient temperature.[15a] A feasible synthetic approach has thus been established for the preparation of a series of triruthenium derivatives containing ortho-metalated 2,2′-bipyridyl ligands. Subsequently, this finding prompted us to attempt cleavage of the ortho C−H bonds with bis-bidentate chelating ligand 2,2′-bipyrimidine (bpym) for preparation of dimeric triruthenium cluster compounds containing bridging bpym in ortho-metalation.[15b] Nevertheless, substitution of a bridging acetate in the parent $Ru_3O(OAc)_6$ core by an ortho-metalated 2,2′-bipyridyl ligand exerts little influence on the electronic and redox characteristics of the triruthenium derivatives.[15]

Azo-aromatic ligands such as 2,2′-azobispyridine (abpy) and 2,2′-azobis(5-chloropyrimidine) (abcp) are π-delocalized bis-bidentate ligands with a very low π^* level and have been widely utilized in the construction of polymetallic complexes that exhibit efficient electronic or magnetic interaction.[16] Inspired by the finding from the substitution of a bridging acetate with an ortho-metalated 2,2′-bipyridyl ligand, we attempt to explore the reactivity of the triruthenium precursor **1** with azo-aromatic bis-bidentate ligands such as abpy and abcp at ambient temperature. As expected, substitution of a bridging acetate in the parent $Ru_3O(OAc)_6$ core by an azo-aromatic ligand occurs indeed, inducing isolation of triruthenium derivatives $[Ru_3O(OAc)_5\{\mu\text{-}\eta^1(N),\eta^2(N,N)\text{-L}\}(py)_2](PF_6)$ (L = abpy (**2**), abcp (**3**)) with the formal oxidation state III,III,II. In contrast strikingly with the slight influence on electronic and physical properties caused by orthometalation of 2,2′-bipyridyl ligands, substitution of a bridging acetate by abpy or abcp modifies dramatically the electronic features and redox properties in the oxo-centered triruthenium derivatives **2** and **3**. Significant anodic shifts of the triruthenium-based redox potentials due to substitution of a bridging acetate in the parent $Ru_3O(OAc)_6$ core by an abpy or abcp ligand results in facile isolation of low-valence $Ru_3^{III,III,II}$ and $Ru_3^{III,II,II}$ species that are usually inaccessible at ambient temperature.[1−6] We describe herein the preparation, characterization, and redox properties of oxo-centered $Ru_3^{III,III,II}$ cluster derivatives $[Ru_3O(OAc)_5\{\mu\text{-}\eta^1(N),\eta^2(N,N)\text{-L}\}(py)_2](PF_6)$ (L = abpy **2**, abcp **3**) together with the one-electron reduced product $Ru_3O(OAc)_5\{\mu\text{-}\eta^1(N),\eta^2(N,N)\text{-abcp}\}(py)_2$ (**3a**) with the formal oxidation state III,II,II.

Experimental Sections

Materials and Reagents. All synthetic operations were performed under a dry argon atmosphere by using Schlenk techniques and vacuum-line systems. Solvents were dried by standard procedures and distilled prior to use. 2,2′-Azobispyridine (abpy) and 2,2′-azobis(5-chloropyrimidine) (abcp) were synthesized by the literature method.[17,18] The parent triruthenium compound $[Ru_3O(OAc)_6(py)_2(CH_3OH)](PF_6)$ (**1**) was prepared by the procedures described in the literature.[1]

$[Ru_3O(OAc)_5\{\mu\text{-}\eta^1(N),\eta^2(N,N)\text{-abpy}\}(py)_2](PF_6)$ (**2**). To a dicholomethane (60 mL) solution of **1** (100 mg, 0.10 mmol) was added abpy (18.4 mg, 0.10 mmol) with stirring at room temperature for 1 d. During the reaction, the solution color changed from blue to green. The product was purified by neutral alumina column chromatography using CH_2Cl_2−MeCN (v/v, 50:1) as an eluent to collect the second green band. Yield: 58%. Anal. Calcd for $Ru_3O_{11}C_{30}H_{33}N_6PF_6$: C, 32.70; H, 3.02; N, 7.63. Found: C, 32.59; H, 3.08; N, 7.66. IR (KBr, cm^{-1}): 1559s (OAc), 1420s (OAc), 842s (PF_6). ESI-MS [*m*/*z* (%)]: 958 (100) $[M - PF_6]^+$.

$[Ru_3O(OAc)_5\{\mu\text{-}\eta^1(N),\eta^2(N,N)\text{-abcp}\}(py)_2](PF_6)$ (**3**). This compound was prepared by the same synthetic procedure as that of **2** using abcp instead of abpy. Yield: 66%. Anal. Calcd for $Ru_3O_{11}C_{28}H_{29}N_8Cl_2PF_6$: C, 28.68; H, 2.49; N, 9.56. Found: C, 28.53; H, 2.83; N, 9.51. IR (KBr, cm^{-1}): 1559s (OAc), 1425s (OAc), 842s (PF_6). ESI-MS [*m*/*z* (%)]: 1028 (100) $[M - PF_6]^+$.

$Ru_3O(OAc)_5\{\mu\text{-}\eta^1(N),\eta^2(N,N)\text{-abcp}\}(py)_2$ (**3a**). To a dichloromethane (50 mL) solution of **3** (117 mg, 0.10 mmol) in an ice−water bath was added a few drops (ca. 0.5 mL) of hydrazine hydrate (20%). After the solution was stirred for half an hour, 10 mL of cold water was added. The dichloromethane layer was separated by an extraction funnel and then washed with 10 mL of cold water. After being separated by extraction, the dichloromethane was removed at reduced pressure. The product was recrystallized by dichloromethane−hexane and dried in vacuo. Yield: 51%. Anal. Calcd for $Ru_3O_{11}C_{28}H_{29}N_8Cl_2$: C, 32.72; H, 2.84; N, 10.90. Found: C, 32.63; H, 2.96; N, 10.57. IR (KBr, cm^{-1}): 1560m (OAc), 1420s (OAc). ESI-MS [*m*/*z* (%)]: 1029 (100) $[M + 1]^+$, 636 (89) $[Ru_3O(OAc)_4(py)]^+$.

(9) (a) Londergan, C. H.; Salsman, J. C.; Ronco, S.; Dolkas, L. M.; Kubiak, C. P. *J. Am. Chem. Soc.* **2002**, *124*, 6236−6237. (b) Londergan, C. H.; Salsman, J. C.; Ronco, S.; Kubiak, C. P. *Inorg. Chem.* **2003**, *42*, 926−928. (c) Zavarine, I. S.; Kubiak, C. P.; Yamaguchi, T.; Ota, K.; Matsui, T.; Ito, T. *Inorg. Chem.* **2000**, *39*, 2696−2698. (d) Londergan, C. H.; Kubiak, C. P. *Chem. Eur. J.* **2003**, *9*, 5962−5969.

(10) (a) Kido, H.; Nagino, H.; Ito, T. *Chem. Lett.* **1996**, *25*, 745−746. (b) Akashi, D.; Kido, H.; Abe, M.; Sasaki, Y.; Ito, T. *J. Chem. Soc., Dalton Trans.* **2004**, 2883−2889.

(11) Ye, S.; Zhou, W.; Abe, M.; Nishida, T.; Cui, L.; Uosaki, K.; Osawa, M.; Sasaki, Y. *J. Am. Chem. Soc.* **2004**, *126*, 7434−7435.

(12) (a) Abe, M.; Sasaki, Y.; Yamaguchi, T.; Ito, T. *Bull. Chem. Soc. Jpn.* **1992**, *65*, 1585−1590. (b) Abe, M.; Sato, A.; Inomata, T.; Kondo, T.; Uosaki, K.; Sasaki, Y. *J. Chem. Soc., Dalton Trans.* **2000**, 2693−2702. (c) Sasaki, Y.; Tokiwa, A.; Ito, T. *J. Am. Chem. Soc.* **1987**, *109*, 6341−6347.

(13) (a) Dovidauskas, S.; Toma, H. E.; Araki, K.; Sacco, H. C.; Iamamoto, Y. *Inorg. Chim. Acta* **2000**, *305*, 206−213. (b) Toma, H. E.; Alexiou, A. D. P.; Dovidauskas, S. *Eur. J. Inorg. Chem.* **2002**, 3010−3017. (c) Nikolaou, S.; Toma, H. E. *Polyhedron* **2001**, *20*, 253−259. (d) Toma, S. H.; Nikolaou, S.; Tomazela, D. M.; Eberlin, M. N.; Toma, H. E. *Inorg. Chim. Acta* **2004**, *357*, 2253−2260. (e) Nikolaou, S.; Toma, H. E. *J. Chem. Soc., Dalton Trans.* **2002**, 352−359.

(14) Chen, J.-L.; Zhang, L.-Y.; Chen, Z.-N.; Gao, L.-B.; Abe, M.; Sasaki, Y. *Inorg. Chem.* **2004**, *43*, 1481−1490.

(15) (a) Chen, J.-L.; Zhang, X.-D.; Zhang, L.-Y.; Shi, L.-X.; Chen, Z.-N. *Inorg. Chem.* **2005**, *44*, 1037−1043. (b) Ye, H.-Y.; Zhang, L.-Y.; Chen, J.-L.; Chen, Z.-N. *Chem. Commun.* **2006**, 1971−1973.

(16) (a) Kaim, W. *Coord. Chem. Rev.* **2001**, *219*−*221*, 463−488 (b) Kaim, W.; Kohlmann, S. *Inorg. Chem.* **1987**, *26*, 68−77. (c) Ernst, S. D.; Kaim, W. *Inorg. Chem.* **1989**, *28*, 1520−1528. (d) Ernst, S.; Kasack, V.; Kaim, W. *Inorg. Chem.* **1988**, *27*, 1146−1148.

(17) Baldwin, D. A.; Lever, A. B. P.; Parish, R. V. *Inorg. Chem.* **1969**, *8*, 107−115.

(18) Doslik, N.; Sixt, T.; Kaim, W. *Angew. Chem., Int. Ed.* **1998**, *37*, 2403−2404.

Table 1. Crystallographic Data for **3**·5$CHCl_3$[a]

empirical formula	$C_{33}H_{34}Cl_{17}F_6N_8O_{11}PRu_3$
formula weight	1769.51
space group	$P\bar{1}$
a, Å	14.370(3)
b, Å	14.595(4)
c, Å	15.995(4)
α, deg	102.835(2)
β, deg	92.410(2)
γ, deg	103.181(3)
V, Å^3	3169.5(13)
Z	2
T (K)	293(2)
ρ_{calc}, g/cm^3	1.854
μ(Mo*K*α),mm^{-1}	1.519
radiation (*λ*, Å)	0.71073
R1 (F_o^2)	0.0527
wR2 (F_o^2)	0.1609
GOF	1.312

[a] $R1 = \Sigma||F_o| - |F_c||/\Sigma|F_o|$, $wR2 = [\Sigma w(F_o^2 - F_c^2)^2/\Sigma w(F_o^2)^2]^{1/2}$.

Crystal Structural Determination. Crystals of **3**·5$CHCl_3$ suitable for X-ray diffraction were obtained by laying hexane onto the dichloromethane−chloroform (v/v, 1:1) solution. A single-crystal sealed in a glass capillary with mother liquor was measured on a MERCURY CCD diffractometer by the *ω* scan technique at room temperature using graphite-monochromated Mo Kα (*λ* = 0.71073 Å) radiation. An absorption correction by SADABS was applied to the intensity data. The structure was solved by direct methods, and the heavy atoms were located from the E-map. The remaining non-hydrogen atoms were determined from the successive difference Fourier syntheses. All the non-hydrogen atoms were refined anisotropically, whereas the hydrogen atoms were generated geometrically with isotropic thermal parameters. The structure was refined on F^2 by the full-matrix least-squares method using the SHELXTL-97 program package.[19] Crystallographic data are summarized in Table 1. Full crystallographic data are provided in the Supporting Information.

Physical Measurements. Elemental analyses (C, H, N) were performed on a Perkin-Elmer Model 240C automatic instrument. Electrospray mass spectra (ESI-MS) were recorded on a Finnigan LCQ mass spectrometer using dichloromethane−methanol as the mobile phase. UV−vis absorption spectra in dichloromethane solutions were measured on a Perkin-Elmer Lambda 25 UV−vis spectrometer. Infrared spectra were recorded on a Magna 750 FT-IR spectrophotometer with KBr pellets. ^{1}H NMR spectra were performed on a Bruker-300 (for **2**) or Bruker-500 (for **3**) in CD_3CN solutions with $SiMe_4$ as the internal reference. The magnetic susceptibility of the powdered sample was measured in a field of 1000 Oe at the temperature range 2−300 K using a SQUID magnetometer. The cyclic voltammogram (CV) and differential pulse voltammogram (DPV) were made with a Princeton Applied Research Potentiostat/Galvanostat 263A in acetonitrile solutions containing 0.1 M $(Bu_4N)(ClO_4)$ as supporting electrolyte. CV was performed at a scan rate of 100 mV s^{-1}. DPV was measured at a rate of 20 mV s^{-1} with a pulse height of 40 mV. Platinum and glassy graphite were used as counter and working electrodes, respectively, and the potentials were measured against an Ag/AgCl reference electrode. The potential measured was always referenced to the half-wave potentials of the ferrocenium/ferrocene ($E_{1/2} = 0$) couple.

(19) Sheldrick, G. M. *SHELXL-97, Program for the Refinement of Crystal Structures*; University of Gottingen: Gottingen, Germany, 1997.

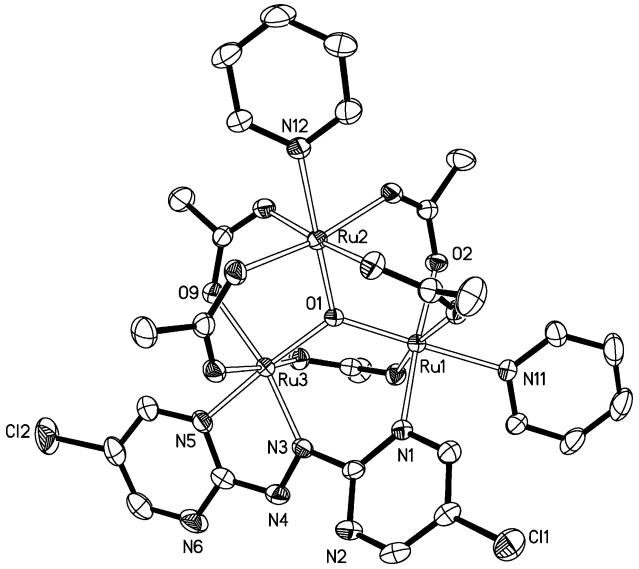

Figure 1. ORTEP drawing of the complex cation of **3** with an atom-labeling scheme showing 30% thermal ellipsoids.

Results and Discussion

Synthesis and Characterization. As shown in Scheme 1, oxo-centered triruthenium cluster derivatives $[Ru_3O(OAc)_5\{\mu\text{-}\eta^1(N),\eta^2(N,N)\text{-}L\}(py)_2](PF_6)$ (L = abpy **2**, abcp **3**) were prepared by reaction of the precursor $[Ru_3O(OAc)_6(py)_2(MeOH)](PF_6)$ (**1**) with 1 equiv of abpy or abcp at ambient temperature. The products are readily purified by alumina column chromatography. Formation of stable $Ru_3^{III,III,II}$ cluster derivatives is involved in the substitution of axially coordinated methanol as well as one of the bridging acetates in the $Ru_3^{III,III,III}$ precursor **1** by an abpy or abcp, in which the formal oxidation state of the triruthenium species is converted from III,III,III to III,III,II. In view of the potential bis-terdentate character for abcp, an attempt to prepare the abcp-linked dimeric $Ru_3O(OAc)_5$ species is unattainable whether by direct reaction of 2 equiv of **1** with abcp or by incorporating **1** with equimolar **3**. Reduction of $[Ru_3^{III,III,II}]^+$ species **3** by hydrazine hydrate induces isolation of one-electron reduced neutral $[Ru_3^{III,II,II}]$ product **3a** which is reversibly oxidizable to **3** by ferrocenium hexafluorophosphate. An attempt to isolate the one-electron reduced product of **2** by addition of zinc amalgam gave an unidentifiable species due to probably the extreme instability.

The microanalytical data for abpy- or abcp-containing triruthenium derivatives accorded well with the theoretical values. The ESI-MS shows that molecular ion fragments $[M - PF_6]^+$ (**2** and **3**) or $[M + 1]^+$ (**3a**) occur as the base peak. The ^{1}H NMR spectra of **2** (Figure 2) and **3** (Figure S4, Supporting Information) show clearly that they are diamagnetic, consistent with the assignment with the formal oxidation state of III,III,II which is verified by single-crystal X-ray diffraction and electrochemical studies (vide infra). The similarity of ^{1}H NMR signals for **2** and **3** demonstrates unambiguously that they have similar structures. By comparison with those observed in diamagnetic parent $Ru_3^{III,III,II}$ compounds $[Ru_3O(OAc)_6(py)_3]$ and $[Ru_3O(OAc)_5\{\mu\text{-}\eta^1(C),\eta^2\text{-}(N,N)\text{-bipyridyl}\}(py)_2]$ with ortho-metalated 2.2′-biyridyl

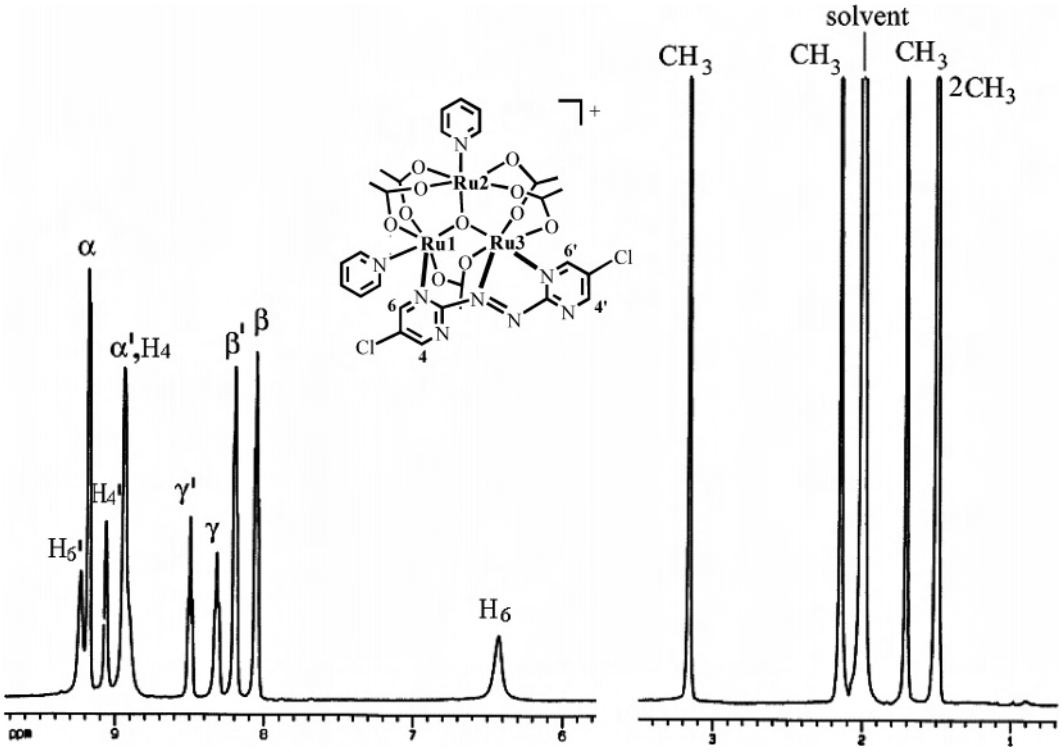

Figure 2. ^{1}H NMR spectrum of **3** in CD_3CN at 298 K.

Scheme 1. Synthetic Routes to **2** and **3**

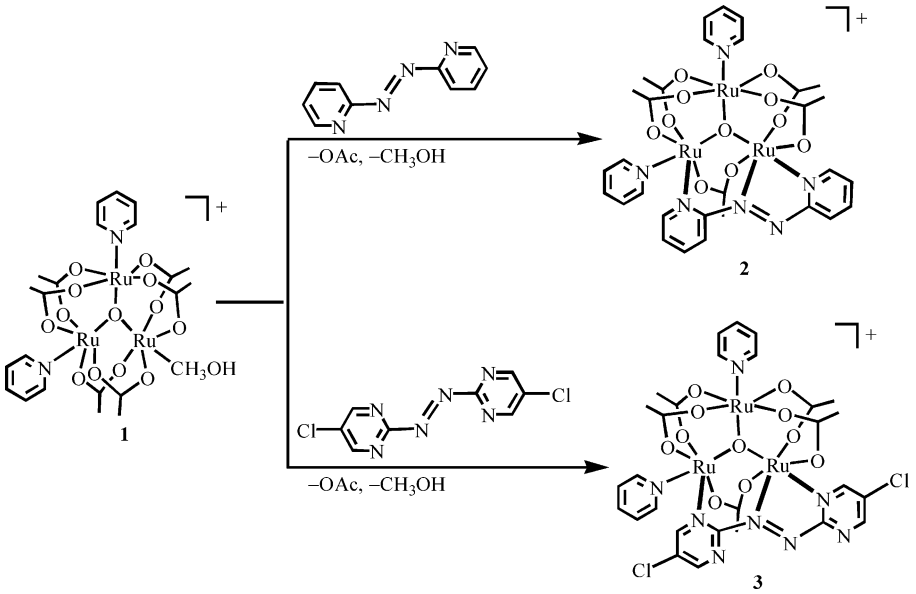

ligands,[1,2,15] the proton signals in **2** (abpy) or **3** (abcp) are tentatively assigned. As indicated in Figure 2, the signals of acetate protons in high field (1.5−3.2 ppm) are recognized readily based on their relative peak intensity. Of the five acetates in **2** or **3**, four acetate signals occur at the normal region (1.2−2.2 ppm), whereas another one exhibits an obvious low-field shift to ca. 3.2 ppm, ascribable to the bridging acetate between Ru1 and Ru3 atoms (Figure 2) which is affected significantly by abpy or abcp coordination. The proton signals of abpy or abcp are comparable to those of the free ligand (8.0−9.3 ppm), except that one (H6) is dramatically high-field shifted to 6.5 ppm for **2** (Figure 2) and 5.9 ppm for **3** (Figure S4, Supporting Information), due to probably a nonbonding interaction between H6 and one acetate oxygen atom.[16c] As revealed by X-ray crystallography, the short O3−H6 distance (2.39 Å) allows the occurrence of a nonbonding interaction.

Variable-temperature magnetic susceptibilities of neutral [$Ru_3^{III,II,II}$] species **3a** (Figure S5, Supporting Information) were measured at the temperature 2−300 K. The magnetic moment is 1.84 μ_B at 300 K, a little higher than the spin-only value (1.73 μ_B) for a single unpaired electron. The μ_{eff} decreased gradually with the temperature decreasing to 0.94 μ_B at 2 K, due to probably the obvious effect of Ru^{III} spin−orbit splitting in the $^2T_{2g}$ ground term as frequently occurring in other Ru^{III} complexes.[20,21]

Table 2. Selected Interatomic Distances (Å) and Bond Angles (deg) for **3**·5CHCl$_3$

		Distances (Å)			
Ru1···Ru2	3.303(3)	Ru1···Ru3	3.331(2)	Ru2···Ru3	3.352(3)
Ru1−O1	1.907(2)	Ru1−O2	2.064(3)	Ru1−O3	2.065(3)
Ru1−O4	2.071(3)	Ru1−N1	2.054(3)	Ru1−N11	2.129(3)
Ru2−O1	1.886(2)	Ru2−O5	2.052(3)	Ru2−O6	2.035(3)
Ru2−O7	2.064(3)	Ru2−O8	2.058(3)	Ru2−N12	2.124(3)
Ru3−O1	1.974(2)	Ru3−O9	2.074(3)	Ru3−O10	2.030(3)
Ru3−O11	2.038(3)	Ru3−N3	1.938(3)	Ru3−N5	2.028(3)
N3−N4	1.319(5)				
		Bond Angles (deg)			
O1−Ru1−N1	91.25(12)	O1−Ru1−O2	92.66(11)	O1−Ru1−O3	94.48(11)
O1−Ru1−O4	95.74(11)	N1−Ru1−N11	90.18(13)	N1−Ru1−O3	88.10(12)
N1−Ru1−O4	93.58(12)	O1−Ru1−N11	178.54(12)	O2−Ru1−N11	85.90(12)
O1−Ru2−O6	94.10(11)	O1−Ru2−O5	91.86(12)	O1−Ru2−O8	94.98(11)
O6−Ru2−O8	91.34(12)	O5−Ru2−O8	87.61(12)	O1−Ru2−O7	95.73(11)
O6−Ru2−O7	87.96(12)	O5−Ru2−O7	91.97(12)	O1−Ru2−N12	179.25(12)
N3−Ru3−O1	98.44(12)	N3−Ru3−N5	77.62(14)	O1−Ru3−N5	175.90(13)
N3−Ru3−O10	91.28(13)	O1−Ru3−O10	92.38(11)	N5−Ru3−O10	86.62(13)
N5−Ru3−O9	89.58(14)	N3−Ru3−O11	95.35(13)	N3−Ru3−O9	67.00(12)
Ru1−O1−Ru2	121.10(13)	Ru1−O1−Ru3	118.25(13)	Ru2−O1−Ru3	120.55(13)

Structure of 3. The ORTEP drawing of the complex cation of **3** is depicted in Figure 1. Selected atomic distances and bonding angles are presented in Table 2. **3** can be regarded as a derivative of the parent compound [$Ru_3O(OAc)_6(py)_3$](PF_6) by substitution of a bridging acetate and an axially coordinated pyridine with an abcp ligand. The intramolecular Ru···Ru distances are 3.303(3), 3.352(3), and 3.331(3) Å for Ru1···Ru2, Ru2···Ru3, and Ru1···Ru3, respectively, comparable to those found in other oxo-centered triruthenium cluster compounds.[6,8c] The Ru−$O_{acetate}$ distances (2.030(3)−2.074(3) Å) are also in the normal ranges. The Ru3−O1 (1.974(2) Å) distance, however, is obviously longer than those of the other two Ru−O_{oxo} (1.886(2) and 1.907(2) Å) bonds, arising probably from the influence of the trans effect of the shorter Ru3−N5 (2.028(3) Å) bond compared with those of the corresponding Ru1−N1 (2.129 Å) and Ru2−N2 (2.124(3) Å) bonds (vide infra).

As shown in Figure 1, the abcp exhibits a μ-η^1(N),η^2(N,N) bonding mode, chelating the Ru3 center via azo N3 and the pyrimidine N5 donor as well as bound to the Ru1 center via the N1 donor in the other pyrimidine ring. The $Ru_3O(AcO)_5$-(μ-η^1(N),η^2(N,N))$(py)_2$ cluster structure is thus stabilized by formation of a five-membered and a six-membered coordination ring arising from abcp in μ-η^1(N),η^2(N,N) bonding fashion. It is noteworthy that the Ru3−N5 bond is at the axial site of the Ru3 octahedron, whereas azo N3 and the pyrimidine N1 donor are situated on the equatorial plane of the Ru1 octahedron, in which N3 and N5 donors function as the substituted bridging acetate O donors. It is reasonable that the axial Ru3−N5 (2.028(3) Å) distance is longer than that of the equatorial Ru3−N3 (1.938(3) Å) in the five-membered chelating ring. The chelating effect induces a significantly shorter axial Ru3−N5 (2.028(3) Å) length relative to those of the other two axial Ru−N_{pym} (Ru1−N11 = 2.129 Å, Ru2−N12 = 2.124(3) Å). The distance differences (0.116 and 0.090 Å) between the Ru−N_{azo} (Ru3−N3 = 1.938(3) Å) and the Ru−N_{pym} (Ru1−N1 = 2.054(3) Å and Ru3−N5 = 2.028(3) Å) bonds are larger than those found in [(μ-abpy){$Ru(acac)_2$}$_2$] (0.055 Å)[22] and [Pt(abpy)-Cl_2]$_2$[$ZnCl_2$] (0.083 and 0.043 Å)[23] but smaller than that in [Os_4(μ-H)$_4$$(CO)_{10}$(abpy)] (0.129 Å).[24] The pyrimidine-N═N-pyrimidine array is trans-oriented as in most of the abpy and abcp complexes.[18] The azo N═N (N3−N4 = 1.319(5) Å) distance is the normal range (1.26−1.37 Å) as found in other metal complexes.[16,18] The torsion angle of C4−N3−N4−C5 is 164.6°.

Electronic Absorption Spectra. The UV−vis spectral data of **2**, **3**, and **3a** in dichloromethane at 298 K are summarized in Table 3. The electronic absorption spectra of **3** and one-electron reduced product **3a** are depicted in Figure 3. High-energy absorption bands in the ultraviolet region are assigned to $\pi \rightarrow \pi^*$ transitions of the ligand-centered transitions. The absorption shoulders at 340−500 nm with medium energy are sensitive to the oxidation states as well as the axial ligands, induced likely by cluster-to-ligand charge transfer (CLCT) transitions[1,2] from the occupied dπ orbitals of the triruthenium cluster core to the lowest unoccupied π^* orbitals of the ligands.[6] The moderate cluster-to-ligand charge-transfer absorptions suggest that N-heterocyclic π^* interactions with the metal dπ orbitals in these triruthenium compounds are not significant.

In the visible to near-infrared region (600−1000 nm), two broad composite bands originate likely from intracluster (IC) transitions which are characteristic of oxo-centered Ru_3O clusters with delocalized electronic structures.[1,6,15] These low-energy bands are highly dependent on the electron content or formal oxidation states of the Ru_3O clusters.[1,2c,6] A qualitative molecular orbital scheme was proposed by Cotton and Norman[25] and then applied by Baumann and Meyer[1,2] to interpret the electronic structures of triruthenium cluster

(20) Bai, L. X.; Liu, X.; Wang, W. Z.; Liao, D. Z.; Wang, Q. L. Z. *Anorg. Allg. Chem.* **2004**, *630*, 1143.
(21) Harzion, Z.; Navon, G. *Inorg. Chem.* **1982**, *21*, 2606−2608.
(22) Sarkar, B.; Patra, S.; Fiedler, J.; Sunoj, R. B.; Janardanan, D.; Mobin, S. M.; Niemeyer, M.; Lahiri, G. K.; Kaim, W. *Angew. Chem., Int. Ed.* **2005**, *44*, 5655−5658.
(23) Dogan, A.; Sarkar, B.; Klein, A.; Lissner, F.; Schleid, T.; Fiedler, J.; Zalis, S.; Jain, V. K.; Kaim, W. *Inorg. Chem.* **2004**, *43*, 5973−5980.
(24) Li, Y.; Lin, Z.-Y.; Wong, W.-T. *Eur. J. Inorg. Chem.* **2001**, 3163−3173.
(25) Cotton, F. A.; Norman, J. G., Jr. *Inorg. Chim. Acta* **1972**, *6*, 411−419.

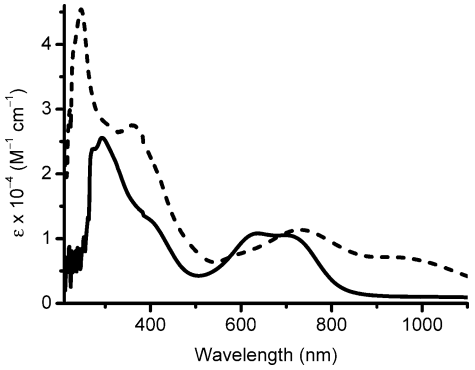

Figure 3. Absorption spectra of **3** (solid) and **3a** (dashed) in dichloromethane.

compounds $[Ru_3O(OAc)_6L_3]^{n+}$ and $[Ru_3O(OAc)_6L_2L']^{n+}$ (n = 2, 1, 0) with D_{3h} and C_{2v} symmetry, respectively. According to this molecular orbital diagram, variations in the electron contents and oxidation states in $[Ru_3O(OAc)_6L_3]^{n+}$ would change the level of molecular orbitals as well as the extent of dπ-pπ interaction, thus causing noticeable red or blue shifts of the low-energy IC bands. As shown in Figure 3, relative to those of $[Ru_3^{III,III,II}]^+$ compound **3** (639 and 702 nm), the absorptions due to IC transitions are significantly red-shifted in one-electron reduced neutral $[Ru_3^{III,II,II}]$ species **3a** (734 and 946 nm). The decrease in energy for these transitions with one-electron reduction reflects the rise of the occupied dπ levels as the electron number increases.[1,2,6] Compared with the low-energy IC bands in **2** (651 and 718 nm), those in **3** (639 and 702 nm) show a shift to higher energy, originating probably from the better π-accepting character for abcp relative to those for abpy as well as the stronger dπ-pπ interaction in abcp compound **3**.

Electrochemistry. Redox chemistry of **2** and **3** was investigated by cyclic and differential pulse voltammetry. Plots of cyclic and differential pulse voltammograms in 0.1 M acetonitrile solutions of $(Bu_4N)ClO_4$ at ambient temperature are shown in Figure 4. Five distinct reversible or quasi-reversible redox waves are observed in the potential range of +1.5 to −2.0 V, in which waves A and B occur in the anodic range, whereas waves C, D, and E occur in the cathodic side. The reversible wave D ($E_{1/2}$ = −1.33 V for **2** and −0.99 V for **3**) is ascribable to the reduction of coordinated abpy or abcp, because the free ligand undergoes the same reduction process at a similar potential range under the same measurement conditions.

With reference to the previous studies on a series of ligand-substituted oxo-centered triruthenium species,[1−15] waves A, B, C, and E correspond most probably to the redox processes $Ru_3^{III,III,IV}/Ru_3^{III,III,III}$, $Ru_3^{III,III,III}/Ru_3^{III,III,II}$, $Ru_3^{III,III,II}/Ru_3^{III,II,II}$, and $Ru_3^{III,II,II}/Ru_3^{II,II,II}$, respectively. As indicated in Figure 4, the corresponding redox potentials in **3** show 0.12−0.30 V positive shifts relative to those in **2** due to probably the better π-accepting capability for pyrimidine-containing abcp than that for pyridyl-containing abpy. As the reduction potential (vs Fc/Fc^+) of the process $Ru_3^{III,III,II}/Ru_3^{III,II,II}$ in **2** (−0.76 V) is 0.30 V higher than that in **3** (−0.46 V), the stable $Ru_3^{III,II,II}$ species **3a** is isolated, whereas the corresponding $Ru_3^{III,II,II}$ species **2a** is inaccessible.

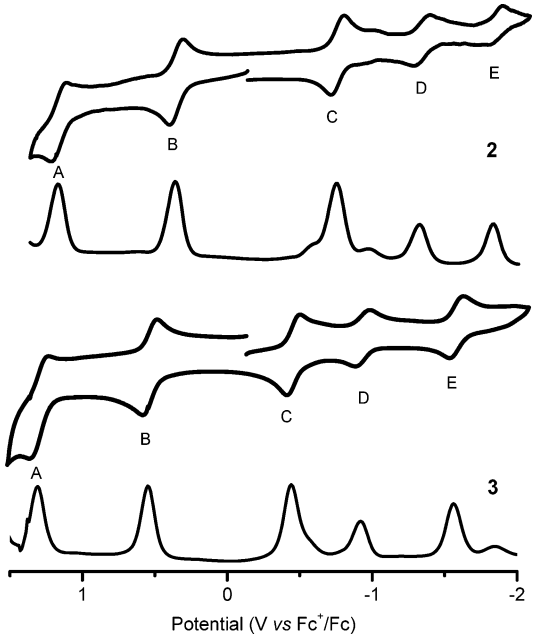

Figure 4. Cyclic and differential pulse voltammograms (CV and DPV) of **2** and **3** in a 0.1 M dichloromethane solution of $(Bu_4N)ClO_4$. The scan rates are 100 mV s^{-1} for CV and 20 mV s^{-1} for DPV.

Compared with those for the parent compound $[Ru_3O(OAc)_6(py)_3](PF_6)$,[1] the corresponding potentials (Table 4) in redox couples $Ru_3O^{III,III,IV}/Ru_3O^{III,III,III}$, $Ru_3O^{III,III,III}/Ru_3O^{III,III,II}$, and $Ru_3O^{III,III,II}/Ru_3O^{III,II,II}$ are positively shifted 0.57, 0.82, and 0.95 V, respectively, for **2**, and 0.69, 0.99, and 1.25 V, respectively, for **3**. The anodic shifts of redox potentials in **2** or **3** are progressively enhanced with a decrease of the formal oxidation states in the triruthenium cluster cores. Such a significant influence on the redox potentials by introducing abpy or abcp to the Ru_3O cluster complexes is much more remarkable than any other used ligands including CO and isocyanide.[1−8,12−15] In our previous study, it has been shown that substituting one of the negatively charged acetates in the parent $Ru_3O(OAc)_6$ core by an anionic 2,2′-bipyridine through ortho-metalation causes little influence on the electronic and redox characteristics of the triruthenium compounds.[15] Consequently, using π-delocalized neutral ligands such as abpy and abcp to substitute one of the negatively charged acetates in the parent $Ru_3O(OAc)_6$ core modifies significantly triruthenium-based redox potentials relative to the parent triruthenium compound $[Ru_3O(OAc)_6(py)_3](PF_6)$.[1]

The effects of axial ligands on the electrochemical behavior of oxo-centered triruthenium cluster species have been systematically investigated.[1,6,7,8c] It has been demonstrated that redox potentials of the triruthenium clusters with the general formula $[Ru_3O(OAc)_6L_3]^+$ are determined by both σ-donation ability and π-back-bonding effect of the axial ligands. On one hand, high formal oxidation states in the oxo triruthenium species are stabilized as the σ-donor strength of an axial ligand increases. On the other hand, π-back-bonding effect favors stabilization of the low oxidation states.[7] Both abpy and abcp are characterized by

Table 3. Absorption Spectral Data for **2**, **3**, and **3a** in Dichloromethane

	λ_{max}/nm (ϵ/M^{-1} cm^{-1})			
complex		IC[a]	CLCT[b]	ligand-centered transitions
2	718 (11300)	651 (10720)	390sh (13000)	322 (23260), 269 (21530)
3	702 (10500)	639 (10800)	410sh (11980)	294 (25660), 273 (23650)
3a	946 (7280)	734 (11500)	425sh (19220)	246 (45300)
			368 (27600)	

[a] IC is intracluster transition. [b] CLCT is cluster-to-ligand charge transfer.

Table 4. Electrochemical Data[a] of **2**, **3**, and Related Oxo-Centered Triruthenium Compounds

complex	$E_{1/2}$ (A) ($Ru_3^{III,III,IV}$/$Ru_3^{III,III,III}$)	$E_{1/2}$ (B) ($Ru_3^{III,III,III}$/$Ru_3^{III,III,II}$)	$E_{1/2}$ (C) ($Ru_3^{III,III,II}$/$Ru_3^{III,II,II}$)	$E_{1/2}$ (D) (L/L^{-1})	$E_{1/2}$ (E) ($Ru_3^{III,II,II}$/$Ru_3^{II,II,II}$)
2	+1.17	+0.36	−0.76	−1.33	−1.84
3	+1.29	+0.53	−0.46	−0.99	−1.58
$[Ru_3O(OAc)_6(py)_3](PF_6)$[b]	+0.60	−0.46	−1.71		
$[Ru_3O(OAc)_5(py)_2(bpy)](PF_6)$[c]	+0.53	−0.62	−1.97		
$Ru_3O(OAc)_6(py)_2CO$[b]	+0.89	+0.25	−1.25		
$[Ru_3O(OAc)_6(2\text{-mpyr})_3](PF_6)$[b]	+0.74	−0.27	−1.40		
$Ru_3O(OAc)_6(CNXy)_3$[d]	+0.94	−0.01	−0.67		

[a] Potential data in volts vs Fc^+/Fc are from single scan cyclic voltammograms recorded in acetonitrile at 25 °C. Detailed experimental conditions are given in the Experimental Section. [b] The data are from ref 1. [c] The data are from ref 15a. [d] The data are from ref 8c.

extremely low-lying π^* orbitals which undergo even further stabilization by metal coordination.[16] This feature induces very favorable orbital overlapping between dπ orbitals of the Ru_3O cluster and π^* orbitals of abpy or abcp. By comparison of the corresponding pK_a values, it appears that the σ-donation ability of abpy or abcp is comparable to that of 2-methylpyrazine (2-mpyr).[6,7,16b] Nevertheless, the corresponding redox potentials of **2** or **3** are more positive by 0.40−0.90 V compared with those of $Ru_3O(OAc)_6(2\text{-mpyr})_3$,[1] revealing distinctly a significant contribution from π-back-bonding effects for abpy (**2**) or abcp (**3**) complexes. CO is a well-known strong π-electron acceptor, which induces the redox potentials in $Ru_3O(OAc)_6(py)_2(CO)$ to exhibit considerable large positive shifts (0.40−0.50 V) compared with those in the parent $[Ru_3O(OAc)_6(py)_3](PF_6)$ because of the remarkable π-back-bonding effects from CO.[1] As listed in Table 4, the corresponding redox potentials in **2** or **3** are obviously more positive than those in $Ru_3O(OAc)_6(py)_2(CO)$[1] and $Ru_3O(OAc)_6(py)_2(CNR)_3$,[8] demonstrating clearly that abpy and abcp are even more efficient for stabilization of low-valence in the oxo-centered triruthenium compounds compared with those of CO or isocyanides. Alternately, since 2,2′-bipyrimidine (bpym) is also featured with very low-lying π^* orbitals,[16b] it is anticipated that substitution of a bridging acetate in the parent $[Ru_3O(OAc)_6(py)_3](PF_6)$ would cause a significant influence on electronic character and redox potentials. Nevertheless, the experimental data reveal unambiguously that the electronic and redox chemistry in the bpym-substituted compounds[15b] $[\{Ru_3O(OAc)_5(py)_2\}(bpym)](PF_6)$ and $[\{Ru_3O(OAc)_5(py)_2\}_2(\mu_4\text{-bpym})](PF_6)_2$ is slightly modified because of the ortho-metalation of deprotonated mono- and dicationic 2,2′-bipyrimidine which results in a slight influence on the dπ and π^* orbital energy.

Summary

A synthetic approach is established for preparation of low-valence oxo-centered triruthenium cluster derivatives at ambient temperature via substitution of a bridging acetate in the parent $Ru_3O(OAc)_6$ cluster core by 2,2′-azobipyridine or 2,2′-azobis(5-chloropyrimidine) in the μ-η^1(N),η^2(N,N) bonding mode. From structural and spectroscopic characterization, it is demonstrated that a bridging acetate substitution by a neutral abpy or abcp affects significantly the electronic and redox characteristics of the oxo-centered triruthenium cluster compounds. The abpy- or abcp-substituted oxo-centered triruthenium derivatives exhibit a high stabilization on low-valence III,III,II and III,II,II species which are usually unavailable through axial ligand-substitution reactions. The synthetic strategy described herein opens a significant approach to tune the redox levels of oxo-centered triruthenium cluster units for the design of multifunctional materials.

Acknowledgment. This work was supported financially by the NSFC (Grants 90401005, 20490210, 20521101, and 20625101), the NSF of Fujian Province (E0420002), and the Key Project from CAS.

Supporting Information Available: Figures with ESI-MS of **2**, **3**, and **3a**, ^{1}H NMR spectrum of **2**, and CIF file of the X-ray crystallographic data for **3**. This material is available free of charge via the Internet at http://pubs.acs.org.

IC0702771